



LAWRENCE
LIVERMORE
NATIONAL
LABORATORY

Pressure Model for the Vacuum System for the Electron Gun and Injector for LCLS Final Design Report

L. S. Tung, L. Eriksson

May 9, 2006

Disclaimer

This document was prepared as an account of work sponsored by an agency of the United States Government. Neither the United States Government nor the University of California nor any of their employees, makes any warranty, express or implied, or assumes any legal liability or responsibility for the accuracy, completeness, or usefulness of any information, apparatus, product, or process disclosed, or represents that its use would not infringe privately owned rights. Reference herein to any specific commercial product, process, or service by trade name, trademark, manufacturer, or otherwise, does not necessarily constitute or imply its endorsement, recommendation, or favoring by the United States Government or the University of California. The views and opinions of authors expressed herein do not necessarily state or reflect those of the United States Government or the University of California, and shall not be used for advertising or product endorsement purposes.

This work was performed under the auspices of the U.S. Department of Energy by University of California, Lawrence Livermore National Laboratory under Contract W-7405-Eng-48.

LLNL/UCRL-XXXX

*Pressure model for the vacuum system for the
electron gun and injector for LCLS*

Final Design Report

Louann Tung
(NTED, LLNL)
and
Leif Eriksson
(LCLS, SLAC)

**Submitted To: LCLS, SLAC
April 28, 2006**



Linac Coherent Light Source

Stanford Linear Accelerator Center

Lawrence Livermore National Laboratory

Table of Contents

1	INTRODUCTION	3
1.1	GENERAL DESCRIPTION.....	3
2	PERFORMANCE SPECIFICATIONS	5
2.1	SYSTEM REQUIREMENTS	5
2.2	VACUUM DESIGN LAYOUT	5
3	DETAILED DESCRIPTION	7
4	NUMERICAL MODEL	9
4.1	GAS LOAD MATRIX.....	9
4.2	CONDUCTANCE ASSUMPTIONS	10
4.3	OUTGASSING RATE.....	10
4.4	PUMP SPEED.....	11
4.5	BENCHMARKS.....	12
5	RESULTS OF THE MODEL	12
5.1	STATIC VALUES.....	12
5.2	TIME-DEPENDENT RESULTS WITH CONSTANT OUTGASSING RATE.....	17
5.3	PUMP FAILURE ANALYSIS	18
5.4	TIME-DEPENDENT OUTGASSING RATE.....	19
6	FUTURE WORK	21
6.1	MODEL IMPROVEMENTS	21
6.2	SUGGESTED TEST	22
	APPENDIX I : IL AND SASL COMPONENT LOCATIONS	23
	APPENDIX II : CODE TO CALCULATE Z VALUES OF COMPONENTS	24

1 Introduction

The vacuum system of the injector for the Linac Coherent Light Source (LCLS) has been analyzed and configured by the Lawrence Livermore National Laboratory's New Technologies Engineering Division (NTED) as requested by the SLAC/LCLS program. The vacuum system layout and detailed analyses for the injector are presented in this final design report. The vacuum system was analyzed and optimized using a coupled gas load balance model of sub-volumes of the components to be evacuated.

1.1 General Description

The injector is comprised of the electron gun, a Gun Spectrometer Line a transport tube containing focusing magnets, diagnostics, and waveguides, an insertion line IL into the SLAC linac, and a straight ahead spectrometer line SASL that ends in a beam dump. The total evacuated length is 25.8 meters. A simple sketch of the vacuum system is shown in Fig. 1.1. There are nine vacuum pump locations and five valves. Light blue indicates the vacuum region that is modeled.

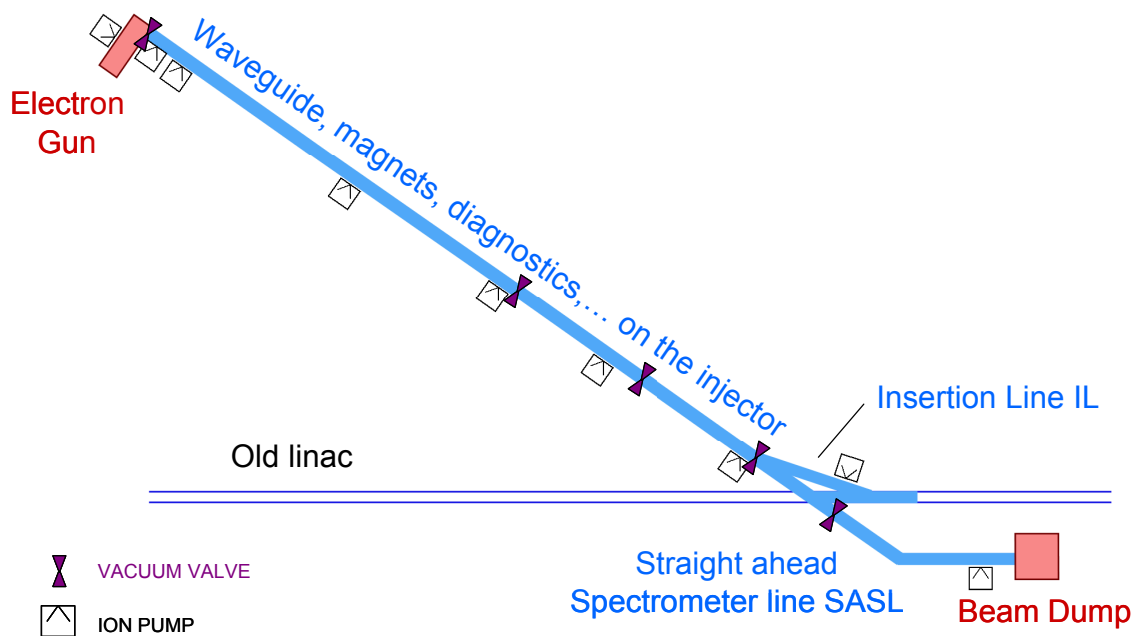


Fig. 1.1. Sketch of the injector vacuum system - the section modeled is shown in blue.

Three-dimensional renderings of the gun and the region where the injector inserts into the linac at the IL and at the SASL are provided in Fig. 1.2 and 1.3.

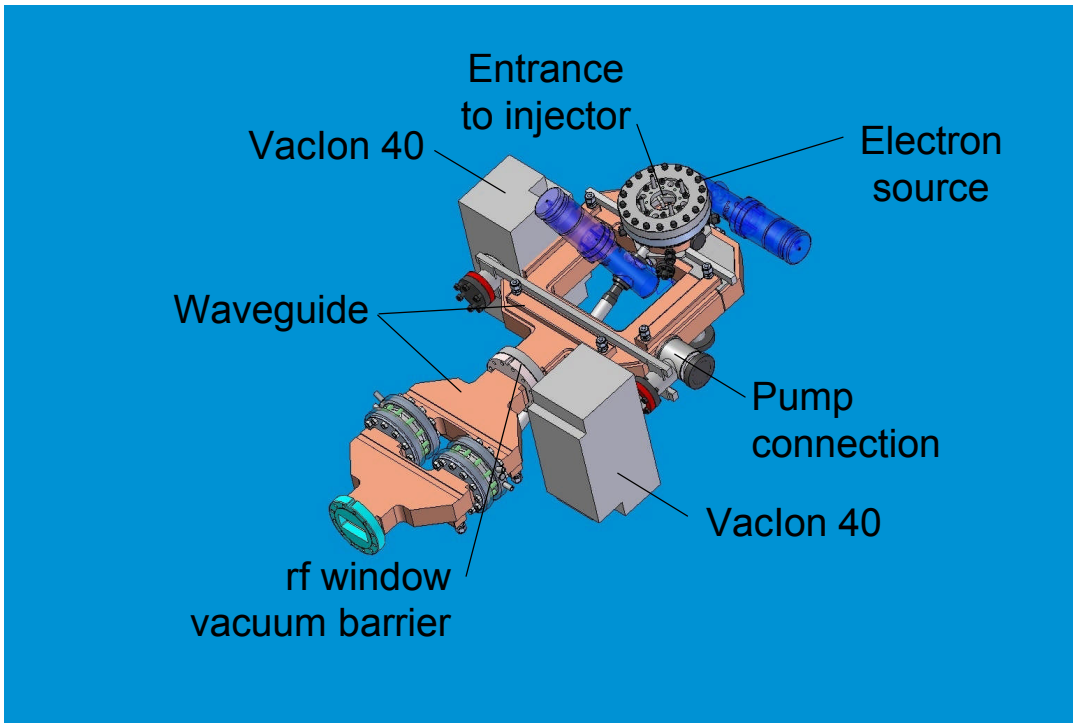


Fig. 1.2. Rendering of the electron gun

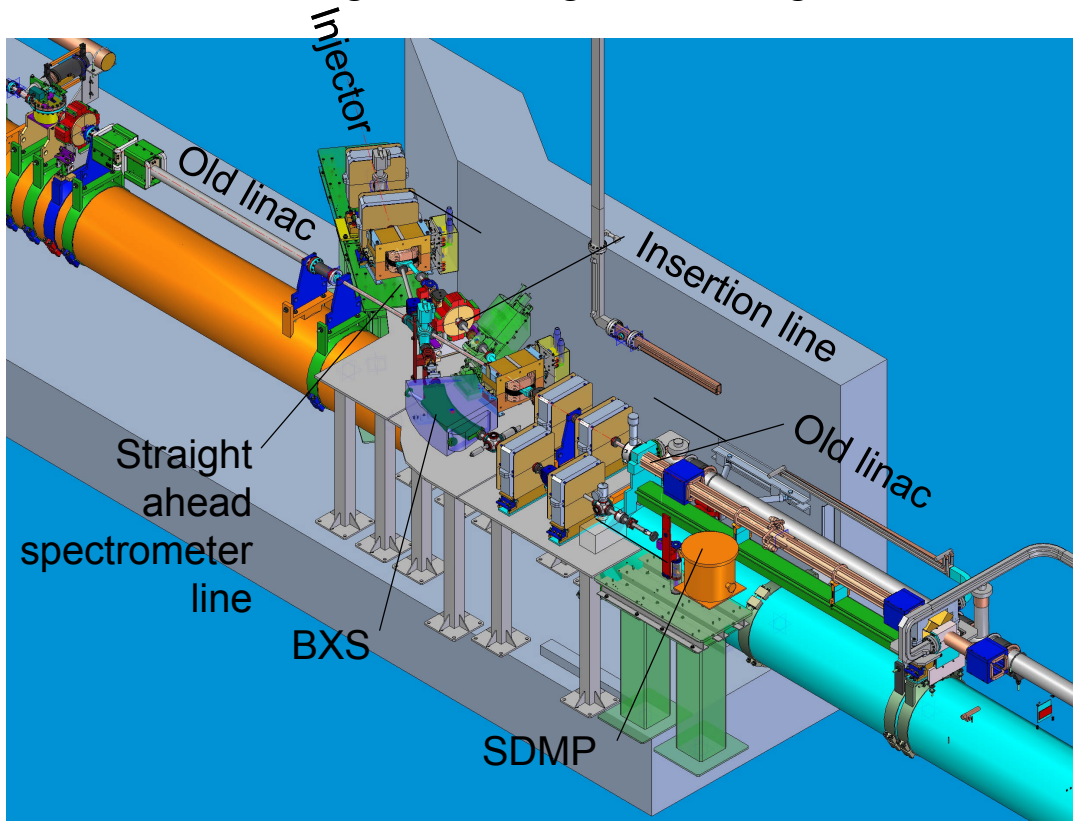


Fig. 1.3. Rendering of the injector near the SLAC linac

2 Performance Specifications

2.1 System Requirements

The primary requirement for the injector vacuum system is to provide sufficient pumping to overcome the surface outgassing rate of the vacuum facing components. All surfaces are assumed to outgas at a rate of 2×10^{-12} Torr-lit/sec/cm². The leak rate of seals and valves were not included as they were considered relatively insignificant. The requirements and the final design values are summarized in Table 2.1. The calculated gun pressure did not meet the design values; however, LCLS vacuum staff felt that it was sufficiently within the pressure range to be acceptable. All pressures in the remaining injector tube were two orders of magnitude below the design value.

PARAMETER		REQUIREMENTS / VALUE
Pumping to overcome system outgassing rate		2×10^{-12} Torr-lit/sec/cm ²
Gun pressure	Design	3×10^{-10} Torr
	Required	1×10^{-10} Torr
Tube pressure	Design	7×10^{-9} Torr (max at the beam dump) 2×10^{-9} Torr (average)
	Required	$< 5 \times 10^{-7}$ Torr

Table 2.1. Injector System Requirements

2.2 Vacuum design layout

Turbo pump carts pump the system down to 10^{-6} Torr. Then carts are removed and Varian VacIon 40's and 20's noble diode ion pumps evacuate the system to the 10^{-9} Torr range and lower. The ion pumps maintain the system pressure for years of operation with minimal maintenance. The design pressure within the gun is in the 10^{-10} Torr range and the design pressure in the remaining system is 5×10^{-7} Torr.

When the turbo carts pumps the system to 10^{-6} Torr, the outgassing rate of the internal surfaces is assumed to be a constant 2×10^{-12} Torr. Described later in this report, we also conduct a study of time-dependent effects that would occur during commissioning. During the first pump-down, the outgassing rate will slowly decrease; hence, we also analyze the pressure response when the outgassing rate drops from 1×10^{-11} Torr-lit/s/cm² to 2×10^{-12} Torr-lit/s/cm² over one day.

A sketch of the vacuum system and pump layout is shown in Fig. 2.1. There are 13 ion pumps in 9 locations. Varian VacIon ion pumps with a nominal speed of 40 lit/s (except two at P2 that are 20 lit/s) are placed in the Gun and along the tube wherever space allows. Pumps in locations P1-P6 are connected with an arm (seen in Fig. 1.2) and "shower drain" (a 7 slit aperture to stop the rf propagation into the pump). Pumps in locations P7-P9 are connected only with a 1.5" Varian Tee. There are five valves labeled VV01 through VV05 that can isolate the injector sections in case of leaks. (Valve VV05 in Fig. 4 is the same as VVSI in the LCLS drawings.)

The gun entrance is referenced as $z = 0$. Distances from each component to the gun were calculated from the x-y coordinates from the drawing #SD380-020-06 (checked 11-18-05), element list, emailed drawing in App. I and emails from Leif Eriksson dated Dec. 2005 through Feb. 2006. Beyond the gun, the tube has an ID of 1.37" for $z < 2.156$ m and 0.87" for $z > 2.156$ m. There are 25.8 meters of injector tube analyzed in our gas load model.

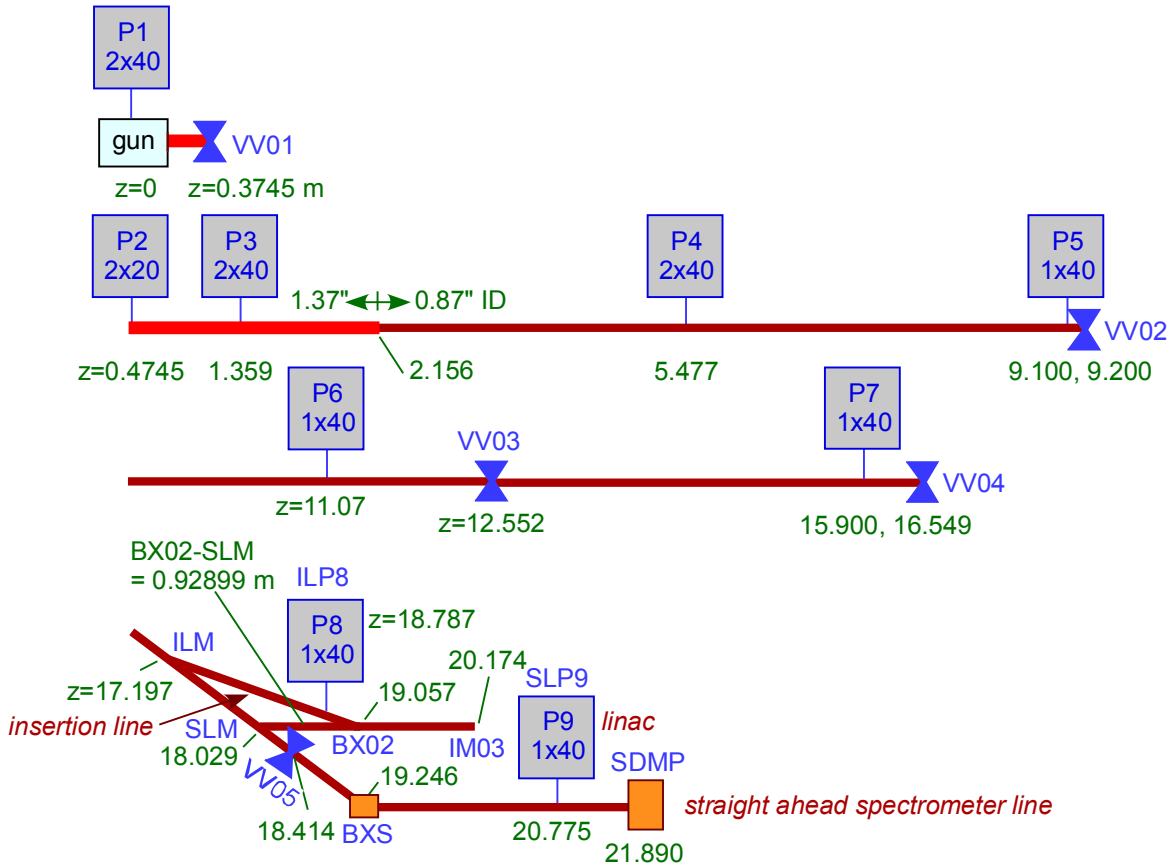


Fig. 2.1. Layout of the LCLS Injector vacuum system.

3 Detailed description

Details of the gun are shown in Fig. 3.1. Each color represents one discrete element or sub-volume in the vacuum model. There are actually 4 sub-volumes but the problem can be reduced to three by symmetry. Node 1 includes the volumes and surface areas of the “Y” waveguide (in blue) and the two alumina rf windows. Node 2 (in yellow) includes the volumes and surface areas of the rectangular “O” of the waveguide and the two connections to the ion pumps. Node 3 (in purple) describes the small details within the electron gun. Node 3 connects to the remaining components of the injector. Also shown are the conductances between nodes (described in more detail later) where C_{wg} , C_{iris} , C_{arm} , and C_{sd} refers to the conductance of the waveguide (1/4 of the perimeter), iris (opening to the gun), arm (pump to waveguide elbow), and shower drain, respectively.

The internal surface area and volume of the vacuum system was calculated for the tube section. The surface area and volumes of the remaining components was provided by SLAC. These values including the gun region components are summarized in Table 3.1.

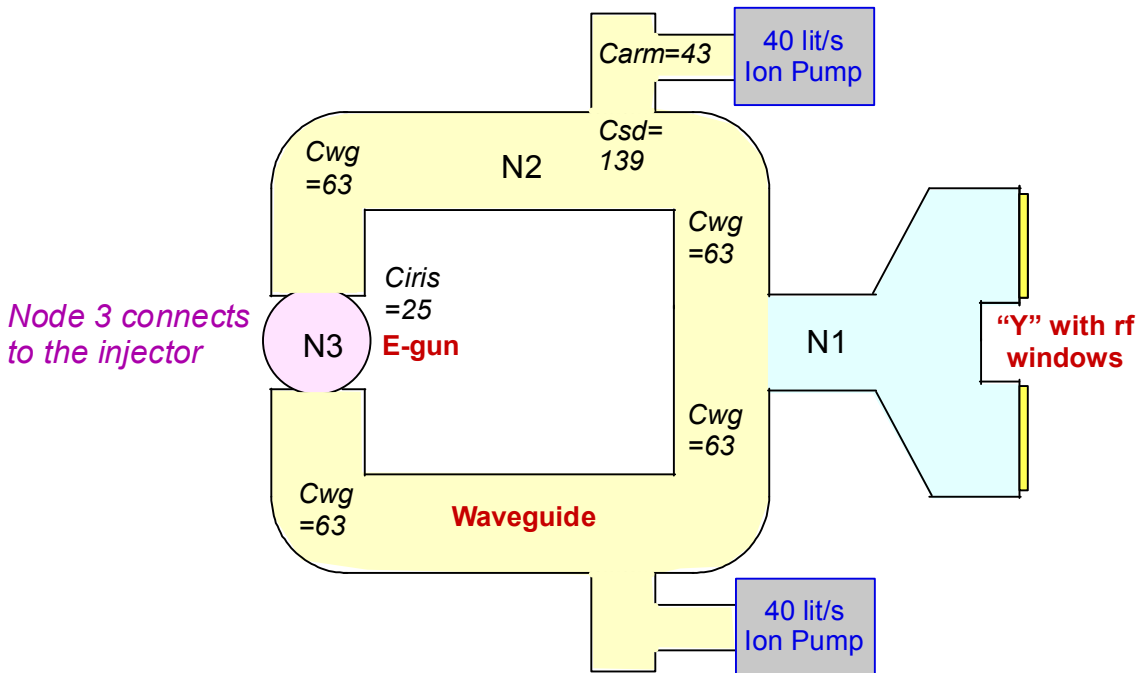


Fig. 3.1. Sketch of electron gun and waveguide section to show the breakdown of the geometry into 3 nodes to model in the gas load matrix.

GUN REGION

GUN (cavity + back space)

Volume = 22.808 + 7.558 in³

Area = 63.134 + 66.219 in²

SQUARE WAVEGUIDE

Volume = 158.178 in³ = 2.592 lit

Area = 353.444 in² = 2280 cm²

Width = 2.84 in

Thickness = 1.34 in

Y WAVEGUIDE + RF WINDOWS

Volume = 67.57 in³

Area Cu = 134.28 in²

Area SS = 4.55 in²

Area two rf windows = 17.45 in²

IRIS at gun entrance

Diameter = 0.65 in

SHOWER DRAIN between waveguide and pump arms

7 slots each composed of 1 rectangle (0.25 “ x (1.26-0.25)”) and two half-circles (0.25” Dia.)

ARMS connecting waveguide to pumps

Dia Arm1 = 1.62” Length Arm1 = 3.71”

Dia Arm2 = 2.26” Length Arm2 = 2.85” (scaled from drawing pg 1)

INJECTOR REGION

INJECTOR DIAMETER

ID = 1.37” for z < 2.156 m ID = 0.87” for z > 2.156 m

INJECTOR x-y and SUML or z coordinates are listed in App. II.

BXS on SASL (two tubes)

Volume = 2 x 115 cm³

Area = 2 x 208 cm²

SDMP on SASL (beam dump)

Volume = 39,517 cm³

Area = 2696 cm²

Table 3.1. Summary of dimensions provided by SLAC that are used in the model

4 Numerical model

4.1 Gas load matrix

Our numerical model of the vacuum system analyzes the gas load balance using a discrete description using nodes or sub-volumes. These nodes are connected to each other through series conductances. For example, the gun region of Fig. 3.1 can be converted to a nodal model as shown below in Fig. 4.1. Here the conductance between nodes 1 and 2 is $C_{1,2} = 2 C_{wg}$; $C_{2,p} = 2/(C_{arm}^{-1} + C_{sd}^{-1})$; and $C_{2,3} = 2/(C_{iris}^{-1} + C_{wg}^{-1})$. Note that the factor of 2 is because the opposite side of the waveguide that includes the second pump is folded into the first side because of symmetry.

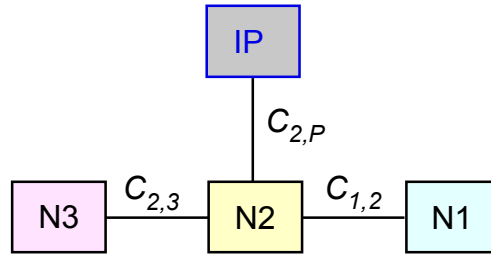


Fig. 4.1. Nodal relationships for the gun region used in the gas load matrix

Pressure history is studied by solving the coupled gas load equations between all the nodes. Mathematica* is used to do the numerical modeling. The outgassing rate is assumed to be constant because the system has been pumped for a long time to reach a constant pressure of 10⁻⁶ Torr. (The results of time-dependent outgassing rate is shown later.) This is the initial condition to solve the gas load matrix. The gas load equations, shown below, are solved simultaneously for all nodes for each timestep until a constant pressure is reached.

$$V_i dp_i/dt = \Sigma Q_{i \text{ in}} - \Sigma Q_{i \text{ out}}$$

where i is the index for the i -th volume,

V is the volume (lit);

dp_i/dt is the rate of change in pressure (Torr/sec);

$\Sigma Q_{i \text{ in}}$ is the sum of surface outgassing or leakage into V_i (Torr-lit/sec);

(surface outgassing is a function of time; O-ring leakage is constant)

and $\Sigma Q_{i \text{ out}}$ is sum of the gas throughput from V_i into V_j ,

$$\text{where } Q_{i \text{ out}} = C_{i \rightarrow j} (p_i - p_j)$$

and $C_{i \rightarrow j}$ is the conductance (lit/sec);

and/or $\Sigma Q_{i \text{ out}}$ is sum of the gas throughput out of V_i ,

* Mathematica 5.2 by Wolfram.

where $Q_{i\ out} = S\ p_i$,
 where S , the effective pump speed (lit/sec), is
 $S = S_p(p_i)\ C_p / (S_p(p_i) + C_p)$,
 where C_p is the conductance between V_i and the pump
 and $S_p(p_i)$ is the pressure dependent pump speed.

4.2 Conductance assumptions

Shape	Conductance (lit/sec)
Long tube	$12.1\ (D^3/L)\ (15\ L/D + 12\ (L/D)^2 + (20+38\ L/D + 12\ (L/D)^2)^\dagger$
Two short tubes with 90° bend	$12.1\ (D^3/(L_1+L_2+ 1.33\ (90/180)D)^\ddagger$
Rectangular duct	$30.9\ a^2\ b^2\ K/((a+b)L + 2.66\ a\ b)^\S$

where L = tube or duct length (cm), D = diameter (cm), a = long side (cm), b = short side (cm), A = area (cm²) and K depends on b/a ^{**}.

The waveguide conductances were based on the formula for a rectangular duct. The length used in the conductance calculation should be the distance between the iris and the pump entrance to the waveguide at the “shower drain”. Since this value is not obvious from the drawings, the value was calculated by using ¼ of the value of the average internal length as based on the total waveguide volume divided by the perimeter = 2 (width + thickness).

The conductance of the shower drain uses the conductance for a rectangular duct rather than an aperture. This shower drain has a thickness of 0.3” which is larger than a slot width of 0.25” so the aperture formula is not valid.

The conductance of the pump arms uses the formula for two short tubes with a 90° bend. The arm with the smaller diameter was used in the formula. Although one tube intersected the second tube midway, the full length of the 2nd tube was used.

4.3 Outgassing rate

The outgassing rate used for all the metal surfaces is 2×10^{-12} Torr-lit/sec/cm². However to account for unknown small areas buried along the tube, we use 2.4×10^{-12} Torr-lit/sec/cm² for all areas outside of the gun ($i \geq 4$). This low rate assumes that the system has been pumped for a long time (days) using turbo pumps. It also assumes that the ion pumps are turned on when the outgassing rate has reached this final constant value.

[†] Roth, A., 1998, Vacuum Technology, (North Holland, Amsterdam) 87.

[‡] *Ibid*, 91.

[§] *Ibid*, 87.

^{**} *Ibid*, 85.

4.4 Pump speed

The VacIon40 Noble Diode pumps have a nominal speed of 40 lit/sec; however, the actual speed depends on pressure as shown in Fig. 4.2. This graph was scanned from the Varian catalog and fit to a formula that is used in the Mathematica model. The pressures near the pumps resulted in an actual pumping speed that varied between 28 and 31 lit/sec.

As observed in previous linacs, the gas composition in the vacuum system is mostly hydrogen;^{††} however, we assume that dry nitrogen is being pumped. The assumption will predict a higher pressure for two reasons. First, the noble ion diode pumps remove hydrogen at a rate that is roughly 1.7 times that of nitrogen. Second, the conductance values are based on the above equations that assume the gas is air (dry nitrogen) at 20° C. Conductances for pure hydrogen would be 3.8 times higher since conductance scales with the square root of the molecular weight. Since the exact composition is unknown and will vary with time, choosing air (dry nitrogen) provides the most conservative pressure calculation.

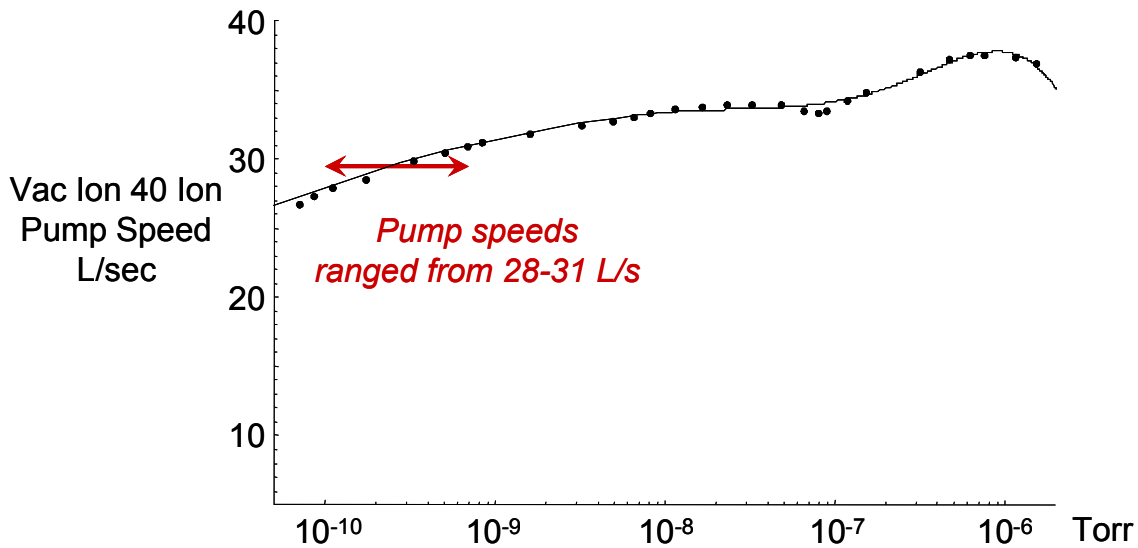


Fig. 4.2. Pressure dependence of pump speed for the VacIon40 Noble Diode ion pump. Dots represent the catalog data. The line represents the numerical fit which is $S(p) = 33.7219 + 120.379 \sin(0.1667 \log(p))^{11} - 42.1059 \sin(0.1682 \log(p))^5 - 2.3765 \sin(0.2196 \log(p))^9$, which is only good for 9×10^{-11} to 2×10^{-6} Torr.

^{††} Liu, Chan and John Noonan, Argonne National Lab/Advanced Photon Source/Technical Bulletin 1995, "Advanced Photon Source Accelerator Ultrahigh Vacuum Guide", 18.

4.5 Benchmarks

The design presented in this report is based on the experience with accelerator projects such as APT/RFQ, APT/LEDA/DTL-CCL^{††}, SNS/DTL-CCL, DARHT II, and SLAC B-Factory. Past applications were models of accelerator cavities connected with apertures. The technique of using this method on long narrow tubes is novel for this design and that of the LCLS/XTOD tunnel thus a benchmark was conducted.

A simple test was run that described a single pump at the end of long tube. The theoretical prediction is that

$$p(x) = q B (L/S + x/C - x^2 / (2CL))^{\dagger\dagger}$$

where q = outgassing rate (Torr-lit/sec/cm²), B = perimeter (cm), S = pump speed (lit/sec), L = length (cm) between the pump and end, and x is the distance from the pump.

The trick was how to divide up a long tube into discrete elements that not only outgas but also restrict the flow of gas. The tube is divided into N discrete sections or sub-volumes. The conductance of each sub-volume is just the total conductance of the tube of length L times the number of sub-volumes. (Applying the conductance formula to individual sub-volumes gave an answer that did not agree with theory.) As N was increased then the solution using the discrete model converged with theory. We found that if the sub-volume length was at least the size of the tube diameter (i.e. SVF > 1), then the model was accurate.

In the injector model, the subvolume length is equal to the twice the smallest tube diameter which has an ID = 0.87". Thus SVF = 2 and $N = 586$. For this case, the run time was 23 sec on a 1.6 GHz PC. When SVF = 0.2 then $N = 5839$ then the run time was 3.4 hours. The system average pressure for both cases was within 0.3%. Thus we have confidence in our discrete model using SVF =2.

5 Results of the model

5.1 Static values

The data from Table 3.1 is transformed into nodal information and summarized in Table 5.1. The total outgassing load is 6.63×10^{-8} Torr-lit/sec. Total nominal pumping speed is 480 lit/sec; however, the total effective pumping speed of the 13 ion pumps is 185.5 lit/sec. This total includes the local pressure dependence of pumping speed and the pump connections. Thus using the simple prediction of $P = Q/S$, then the average pressure is expected to be 3.6×10^{-10} Torr which assumes no conductance loss in the tube.

We chose a subvolume width that is twice the minimum tube diameter. Thus the subvolume width is 2×0.87 ". This subvolume factor SVF of 2 was optimized by comparing the accuracy of the final pressure with runtimes (discussed later). With SVF = 2, the layout of indices is shown in Fig. 5.1. With 3 nodes in the gun section and 25.8 meters of tube and SVF = 2, then the number of nodes is 586. The first 3 indices are with the gun section. Then $i=4$ is the first node in the tube. The indices then follow the tube

^{††} APT LEDA CCDTL Phase 3A PDR Appendix 7A, LLNL/APT 99003.

^{‡‡} Roth, A., 1998, Vacuum Technology, (North Holland, Amsterdam) 133.

through ILM and the insertion line and end at the linac at IM03. The next index starts on the SASL next to the ILM and indices increase along the SASL until the beam dump at SDMP. Finally the last section along the linac is picked up starting with SLM and ending at BX02.

The final plot of the pressure profile is shown in Fig. 5.2. Note in Fig. 5.1, there are nodes at 3 different locations that are connected: where the IL and SASL split at ILM, where the IL meets the linac at BX02, and where the SASL meets the linac at SLM. Thus these three locations have 2 non-sequential nodes that have nearly the same pressures. So one can see on the plot that at ILM that pressures are the same at $i=390$ and 459 ; at BX03 pressures are the same at $i=433$ and 586 ; and at SLM pressures are the same at $i=477$ and 565 .

The gun pressure ($i = 3$) is 3.3×10^{-10} Torr. The minimum pressures are found at the indices closest to the pumps at the nine locations. (See Section 6 for a discussion on pump throat pressures.) The local maxima pressures are in between the pumps with the highest pressure at the beam dump at 7.0×10^{-9} Torr. The system average pressure is 2.2×10^{-9} Torr. This calculated value is 6 times higher than the simple estimate of 3.6×10^{-10} Torr because of the small conductance of the tube. Note that where the tube ends at IM03 and at SLM there is no accounting for pumping beyond this system. Thus the ends are assumed to be sealed. This assumption will give a slightly higher pressure than when this system is connected to the rest of the linac that will provide some additional pumping.

GUN REGION

NODES	Vol, lit	Surface area, cm²
N1, Y + rf windows + 2 arms	1.107	1670
N2, waveguide + 2 arms	2.593	2942
N3, Gun	0.498	835
Total	4.198	5446

CONDUCTANCE between nodes

C_{iris} = 24.8 lit/sec

C_{wg} = 26.4 lit/sec (waveguide quarter length)

C_{sd} = 139.1 lit/sec (shower drain with 7 slots)

C_{arm} = 43.5 lit/sec

C_{2,3} = 2(C_{iris}⁻¹ + C_{wg}⁻¹)⁻¹ = 33.1 lit/sec

C_{2,P} = 2(C_{arm}⁻¹ + C_{sd}⁻¹)⁻¹ = 66.23

C_{1,2} = 2 C_{wg} = 125.1

INJECTOR REGION

NODES	Vol, lit	Surface area, cm²
N1, Y + rf windows + 2 arms	1.107	1008
N2, waveguide + 2 arms	3.217	2785
N3, Gun	0.498	835

CONDUCTANCE between nodes

For z < 2.156 m = 111.7 lit/sec

For z > 2.156 m = 29.40 lit/sec

CONDUCTANCE to pumps & EFFECTIVE PUMPING SPEED if S = 30 lit/sec

For pumps 1-6: C_{arm}/s_d = 33.1 lit/sec S_{eff} = 15.7 lit/sec

For pumps 7-9: C_{tee} = 44.5 lit/sec (Varian Tee) S_{eff} = 17.9 lit/sec

LUMPED VALUES

NODES	Vol, lit	Surface area, cm²	Outgassing rate, Torr-lit/sec
All	57.81	28,401	6.63 x 10 ⁻⁸

Table 5.1. Summary of calculated parameters used in the gas load matrix

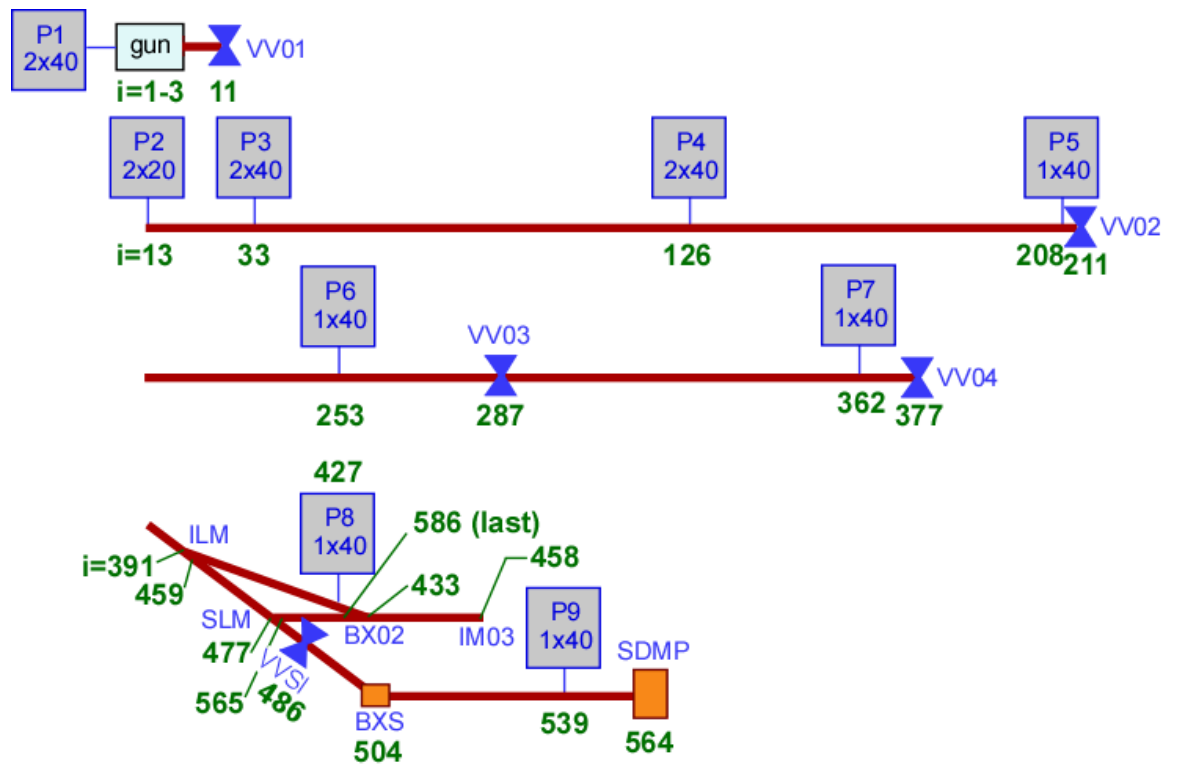


Fig. 5.1. Layout of indices for $N = 586$ generated with $SVF = 2$

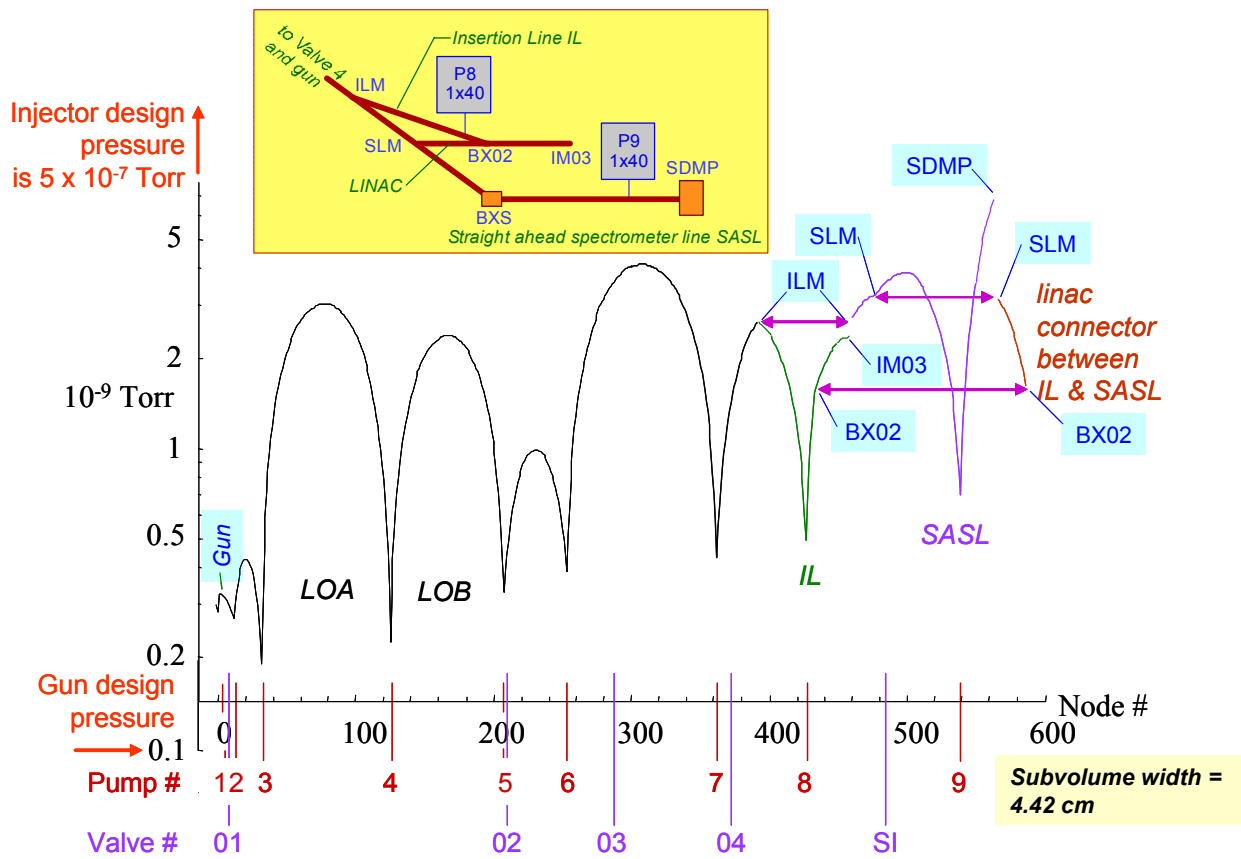


Fig. 5.2. Pressure profile of the entire injector with an outgassing rate of 2×10^{-12} Torr-lit/sec/cm². Inset shows the details of the injector at the IL and SASL. The gun pressure (i=3) is 3.3×10^{-10} Torr. System average pressure is 2.2×10^{-9} Torr. Maximum pressure (at SDMP) is 7.0×10^{-9} Torr.

5.2 Time-dependent results with constant outgassing rate

For the above results, the outgassing rate is set at 2×10^{-12} Torr-lit/sec/cm². Thus the only time-dependent behavior is just the time to pump out the gas in the enclosed volumes. Initially the system pressure is 1×10^{-6} Torr. Plots of the time-history of pressure at the gun and at the beam dump are shown in Fig. 5.3 and Fig. 5.4. The gun pressure equilibrates in 4 seconds and the beam dump by 400 seconds. The beam dump pressure takes considerably longer to equilibrate since its volume is larger and the nearest pump is 1.1 meters away.

Early Gun pressure, Torr

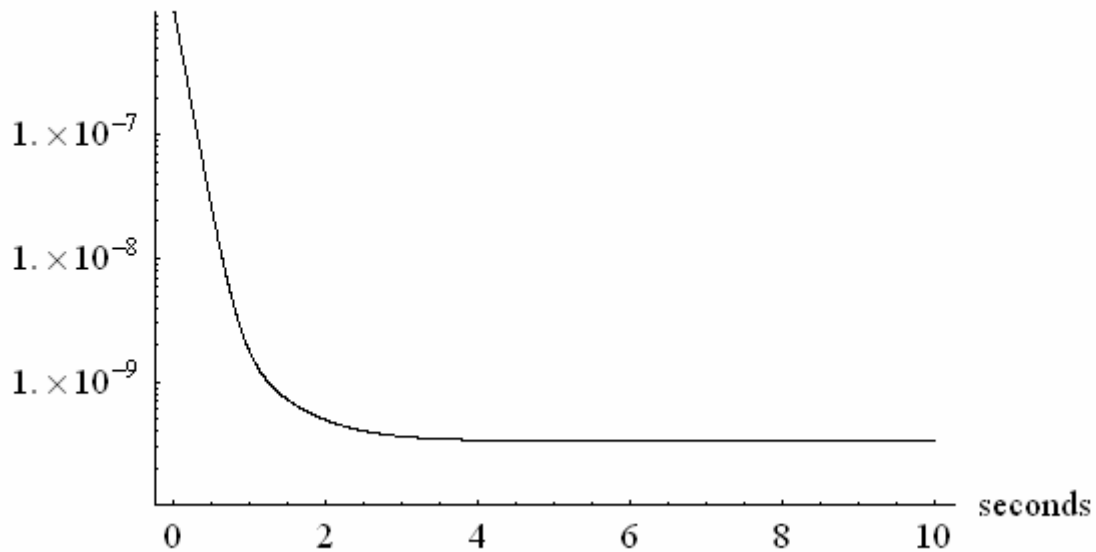


Fig. 5.3. Pressure history at the gun (i=2). Final pressure = 3.3×10^{-10} Torr.

Early SDMP pressure, Torr

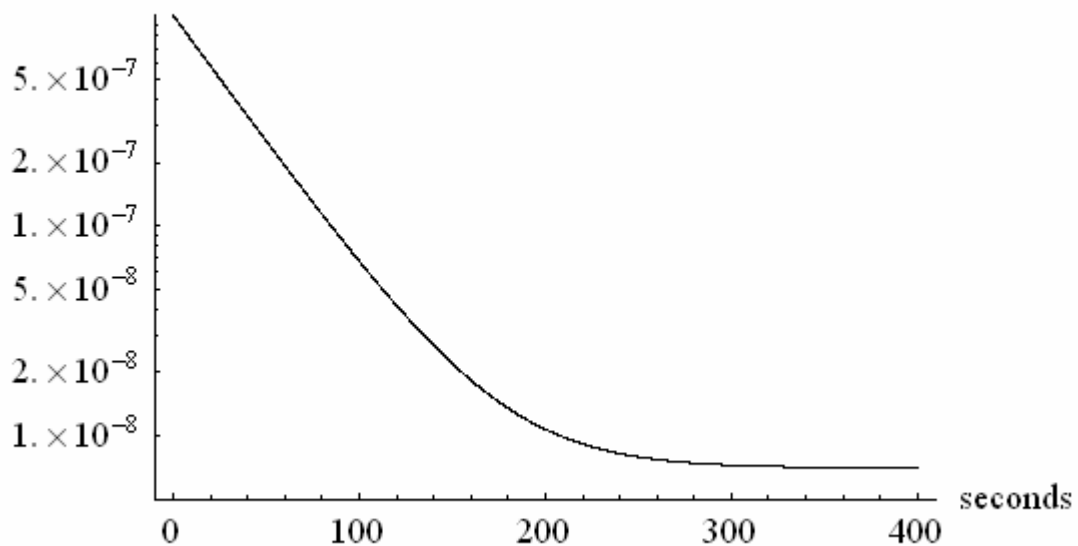


Fig. 5.4. Pressure history at the beam dump (i=564). Final pressure = 7.0×10^{-9} Torr.

5.3 Pump failure analysis

The consequences of the worse case pump failure was also calculated. Since the gun pressure has the least design margin (technically it does not meet the margin), the failures of pumps near the gun is the worse case. Results are summarized below. The failure of a pump at the P2 location ($z = 47.45$ cm, $i = 13$) had less of an impact than the failure of pumps within the gun region. Thus the control systems designer should control the two gun pumps to minimize the likelihood of both failing at once.

MODE	GUN PRESSURE, TORR	MARGIN (DESIGN/CALCULATED)
Normal	3.33×10^{-10}	0.3
One gun pump failed	5.0×10^{-10}	0.2
Both gun pumps failed	5.0×10^{-9}	0.02

Table 5.2. Worse case scenario: consequences of pump failure in the gun region

5.4 Time-dependent outgassing rate

We also conducted a study of time-dependent effects of changing the outgassing rate. The outgassing rate is assumed to vary linearly with time starting at 1×10^{-11} Torr-lit/sec/cm² and ending at 2×10^{-12} Torr-lit/sec/cm² after one day. Thus the outgassing rate used in the code is $q = -9.259 \times 10^{-17} t \text{ (sec)} + 1 \times 10^{-11}$ Torr-lit/sec/cm².

The gun and beam dump locations were monitored to represent the extreme pressures in the system. Results are summarized in Table 5.3. Since the outgassing rate dropped by a factor of 5, the gun and beam dump pressures dropped by a factor of 5. The time to reach these values is immaterial since the pressure will equilibrate in a time that matches the time for the outgassing rate to equilibrate. The time of one day was chosen for convenience.

	t = 400 sec	t = 1 day	function ratio of 400 sec / 1 day
Gun pressure (Torr)	1.61×10^{-9}	3.34×10^{-10}	4.83
SDMP pressure (Torr)	3.49×10^{-8}	7.03×10^{-9}	4.96
Outgassing rate (Torr-lit/sec/cm ²)	9.96×10^{-12}	2.00×10^{-12}	4.98

Table 5.3. Worse case scenario: consequences of pump failure in the gun region

The histories of pressure in the gun and beam dump are shown in Figs. 5.5 and 5.6. Initially the pressure suddenly drops in the time needed to remove the volume of gas at 1×10^{-6} Torr. This time is over 4 sec in the gun and 300 sec in the beam dump. Thereafter the pressure change is then just a function of the outgassing rate. The table below lists the pressures at $t = 400$ sec and $t = 1$ day to compare to the outgassing rates. The last figure shows the pressure profile at $t = 1$ day (at 2×10^{-12} Torr-lit/sec/cm²). The gun is at $i = 3$ and SDMP is at $i = 564$.

Late Gun pressure, Torr

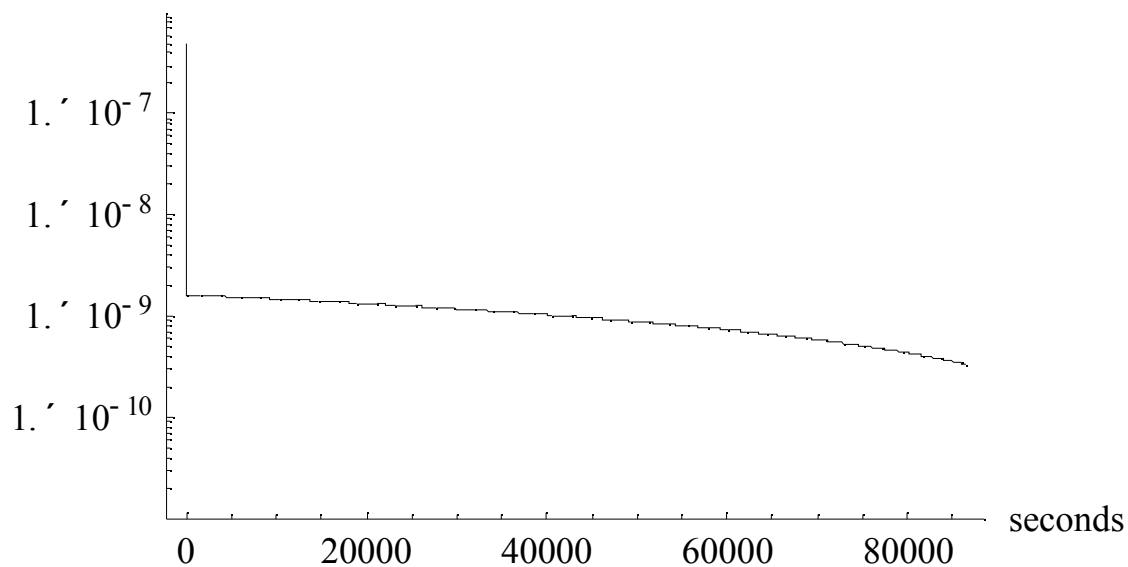


Fig. 5.5. Pressure history at the gun ($i = 3$).

Late SDMP pressure, Torr

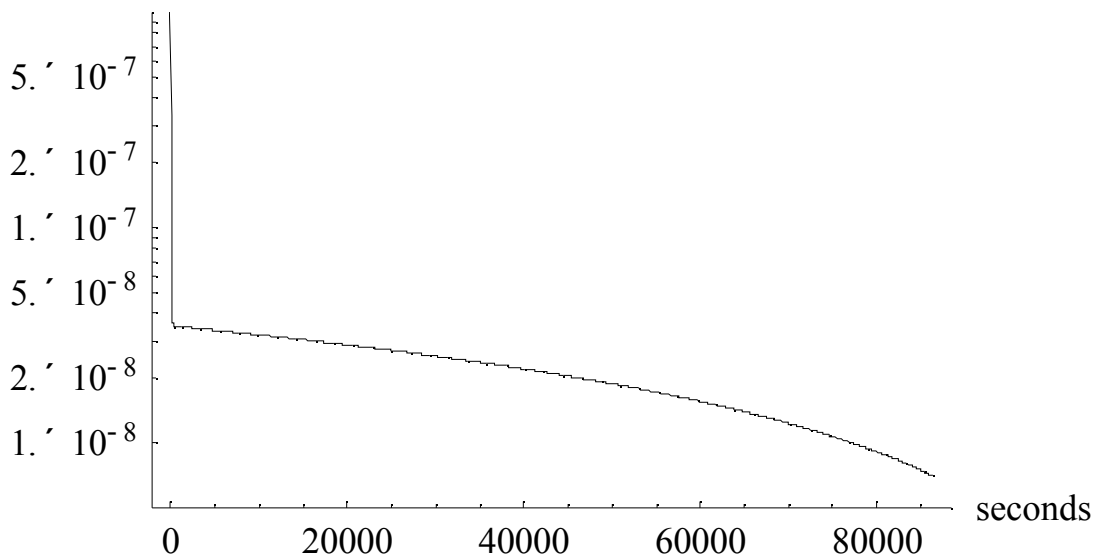


Fig. 5.6. Pressure history at the beam dump ($i = 564$).

6 Future work

6.1 Model improvements

The code has the capability to model time-dependent effects. Thus the gauge locations could be included so that those pressures could be monitored. Then time-dependent effects could be predicted such as pressure response at a gauge due to a failed pump or pressure spike at the gun due to a gauge turning on.

Additional nodes could be added right in front of the pumps. The present model lumps the node right in front of the pump with the node just after the connectors. Thus the actual pump speeds used in the gas load matrix is the effective pump speed. The final calculations will be unaffected but if one would like to compare gauge values with the pressure estimated from the ion currents then an adjustment needs to be made. However this pump pressure can be estimated just with the following formula. Since the actual pump speed is dependent on the throat pressure then using the throat pressure rather than the pressure just outside of the connector would provide a more accurate pump speed. This throat speed would be slightly less than what is presently used. According to Fig. 4.1, a lower throat pressure would result in a lower pump speed so that pressures overall would then increase. We can estimate this change with the following.

At steady state, the gas load balance is just $\Sigma Q_{i \text{ in}} = \Sigma Q_{i \text{ out}}$. With the present model, the connector volume and gas load q_p is added into the nearest node at the tube. If this connector subvolume were treated as a separate node, then pump throat pressure p_p would be related to the pressure p_i on the other side of the connector by

$$p_p = (C_p p_i - q_p) / (S_p(p_p) + C_p)$$

If we use the Varian Tee then $C_p = 44$ lit/sec and $q_p = 213 \text{ cm}^2 \times 2.4 \times 10^{-12} = 5.1 \times 10^{-10}$ Torr-lit/sec. Using Fig. xxx, a typical minimum pressure is 5×10^{-10} Torr. Using Fig. 4.2, then the calculated pump speed is about 30.5 lit/sec. With these numbers, then the throat pressure $p_p = 2.8 \times 10^{-10}$ Torr which is a decrease of about 60% of those minima shown in Fig. xxx. Generally since the connector area is small then $p_i/p_p = S_p(p_p)/C_p + 1$.

This change in calculated throat pressure will change the calculated pumping speed. Referring again to Fig. 4.2, with the pump pressure lower by 60% then the calculated pump speed would drop from 30.5 to 29.2 lit/sec. This speed drop would increase the overall pressure inversely by the same amount that would be 4%. Thus the maximum pressure would increase from 3.3 to 3.4×10^{-10} Torr. This change is in the noise for pressure monitoring. Generally though the smaller the connector conductance then the greater error in throat pressure and pump speed as compared to when the node just in front of the pump is eliminated and effective pump speed is used.

6.2 Suggested test

The two rf windows in the Y in the gun section are assumed to outgas at 2×10^{-12} Torr-li/sec/cm². SLAC microwave staff have stated that, based on their past experience, the rf windows have had an insignificant contribution to the gas load in other linac systems due to the window's bakeout treatment prior to use. Similar but much larger alumina rf windows are in use at LANL. In designing the vacuum system, they assume that the rf window outgasses at 4.5×10^{-9} Torr-lit/sec/cm². This high outgassing rate was measured by ANL (3/1997) for LANL for the alumina rf windows running at 1 MW on the APT/LEDA RFQ. If we use this high rate then the injector gun pressure would be 1×10^{-8} Torr which would be damaging for the gun cathode. The large RFQ windows cannot be baked out in the same way as these gun windows so that the outgassing rates are much higher. However to be sure, I highly suggest that the outgassing rate of the gun windows under rf power are measured prior to installation. Then additional pumping in the gun region could be added if necessary to avoid poisoning the gun cathode. If A Torr-lit/sec/cm² were the new outgassing rate, then roughly the required nominal pumping speed would be $A / (2 \times 10^{-12} \text{ Torr-lit/sec/cm}^2) \times 80 \text{ lit/sec}$ to maintain the same gun pressure of 3×10^{-10} Torr.

Appendix II : Code to calculate z values of components

■ input locations

```
(* In SAB PLAN2.jpg and INS PLAN.jpg,
X dimensions has some unknown
reference.
S dimensions are horizontally referenced to the split point just
upstream of BX01 and Y dimensions are referenced to the Linac -
convert all dimensions from meters to cm. Need (x,y,suml) locations of VV04,
injection line split (ILS), insertion line ion pump P8 (ILP8),
Linac merge point on insertion line at BX02, end of insertion line at IM03,
Linac merge point on Straight-Ahead Spectrometer Line (SSL) (SLM),
VV05 (same as VVSI), bending magnet BXS on SSL (BXS),
ion pump P9 on SSL (SLP9),
beam dump (end of line) on SSL (SDMP). Locations along the insertion
line are from the element chart (hard copy only). Locations along
the spectrometer line are from the e-drawings SAB PLAN2.jpg chart *)

(* BEGIN INPUT *)

VV04SUML = 16.54898603 (* m *); VV04x = 2031.465572 (* m *); VV04y = 0.95825884
(* m *);
BX01deltaY = 1/4 (.7489 -.5413); (* guess from the jpg drawing *);
BX01SUML = 17.29343203 (* m *); BX01x = 2032.08124 (* m *);
BX01s = 0.0812400;
BX01y = 0.5413424 (* m *);
WS04SUML = 18.51722803 (* m *); WS04x = 2033.24396 (* m *); WS04y = 0.16255983
(* m *);
BX02SUML = 19.05702403 (* m *); BX02x = 2033.761324 (* m *);
BS02y = 0.01161378 (* m *);
ILP8SUML = (WS04SUML + BX02SUML) / 2 (* m *); ILP8x = (WS04x + BX02x) / 2
(* m *); ILP8y = (WS04y + BX02y) / 2 (* m *);
(* P8 is midway between BX02 and WS04 *)
IM03SUML = 20.17437003 (* m *); IM03x = 2034.877683 (* m *);
IM03y = -.00000064 (* m *);
(* SLM is midway between XCSI and VVSI (VV05) *)
XCSIs = 0.6484688 (* m *); XCSIy = 0.1299858 (* m *);
VVSI s = 1.0161935 (* m *); VVSIy = -0.1274977 (* m *);
SLMs = (XCSIs + VVSI s) / 2 (* m *); SLM y = 0 (* m *);
BXSs = 1.7289390 (* m *); BXSy = -0.5582677 (* m *);
(* ion pump 9 is half-way between QS02 and MSI *)
SLP9s = (3.0313740 + 3.4837740) / 2 (* m *); SLP9y = -0.6165247 (* m *);
SDMPs = 4.3730200 (* m *); SDMPy = -0.6165247 (* m *);
(* find distance from VV04 to IL-SL split *)
```

```

(* Find distances V4Z (in cm) from VV04 - all x,s (s=0 at ILS),
y (0 at SLM and LCLS), and SUML (along tube length, 0 at gun) values
are in meters *)
(* INJECTOR LINE *)
(* injection line split ILS *)
(* s=0 at ILS on jpg drawings *)

Print [ILSV4Z = (BX01s2 + BX01delta2)0.5 - VV04SUML) 100, " cm = ILS to V4 "]
Print [ILSx = BX01x - BX01s, " m = ILS x component "]
(* injection line ion pump 8 ILP8 *)
Print [ILP8V4Z = (ILP8SUML - VV04SUML) 100, " cm = ILP8 to V4 "]
(* merge to LCLS at BX02 *)
Print [BX02V4Z = (BX02SUML - VV04SUML) 100, " cm = BX02 to V4 "]
(* end of injection line at IM03 *)
Print [IM03V4Z = (IM03SUML - VV04SUML) 100, " cm = IM03 to V4 "]

(* SPECTROMETER LINE *)
(* spectrometer line merge with LCLS at SLM *)
Print [SLMV4Z = 100 (SLMs2 + SLM2)0.5 + ILSV4Z, " cm = SLM to V4 "]
Print [SLMx = SLMs + ILSx, " m = SLM x component "]
(* valve 5 on spectrometer line at VVSI *)
Print [VVSIV4Z = 100 (VVSIs2 + (BX01y - VVSIy)2)0.5 + ILSV4Z, " cm = VVSI to V4 "]
(* bending magnet on spectrometer line BXS *)
Print [BXSIV4Z = 100 (BXSs2 + (BX01y - BXSy)2)0.5 + ILSV4Z, " cm = BXS to V4 "]
(* assume ion pump and beam dump at the same Y value of bending magnet *)
(* spectrometer line ion pump 9 at SLP9 *)
Print [SLP9V4Z = 100 (SLP9s - BXSs) + BXSIV4Z, " cm = SLP9 to V4 "]
(* end of spectrometer line at beam dump SDMP *)
Print [SDMPV4Z = 100 (SDMPs - BXSs) + BXSIV4Z, " cm = SDMP to V4 "]
(* length between BX02 and SLM *)
Print [100 (BX02x - SLMx), " cm = BX02x - SLMx "]
(* length between BX02 and IM03 *)
Print [100 (IM03x - BX02x), " cm = IM03x - BX02x "]
(* length between SDMP and BXS *)
Print [SDMPV4Z - BXSIV4Z, " cm = SDMP - BXS "]

(* SUML for ILS *)
Print [VV04SUML 100 + ILSV4Z, " cm = SUML for ILS "]
(* SUML for SLM *)
Print [VV04SUML 100 + SLMV4Z, " cm = SUML for SLM "]
(* SUML for VV05 *)
Print [VV04SUML 100 + VVSIV4Z, " cm = SUML for VV05 "]
(* SUML for BXS *)
Print [VV04SUML 100 + BXSIV4Z, " cm = SUML for BXS "]
(* SUML for SLP9 *)
Print [VV04SUML 100 + SLP9V4Z, " cm = SUML for SLP9 "]
(* SUML for SDMP *)
Print [VV04SUML 100 + SDMPV4Z, " cm = SUML for SDMP "]
(* SUML for ILP8 *)
Print [VV04SUML 100 + ILP8V4Z, " cm = SUML for ILP8 "]
(* SUML for BX02 *)
Print [VV04SUML 100 + BX02V4Z, " cm = SUML for BX02 "]
(* SUML for IM03 *)
Print [VV04SUML 100 + IM03V4Z, " cm = SUML for IM03 "]

```

64.8043 cm = ILS to V4
2032. m = ILS x component
223.814 cm = ILP8 to V4
250.804 cm = BX02 to V4
362.538 cm = IM03 to V4
148.037 cm = SLM to V4
2032.83 m = SLM x component
186.459 cm = VVSI to V4
269.704 cm = BXS to V4
422.567 cm = SLP9 to V4
534.112 cm = SDMP to V4
92.8993 cm = BX02x-SLMx
111.636 cm = IM03x-BX02x
264.408 cm = SDMP-BXS
1719.7 cm = SUML for ILS
1802.94 cm = SUML for SLM
1841.36 cm = SUML for VV05
1924.6 cm = SUML for BXS
2077.47 cm = SUML for SLP9
2189.01 cm = SUML for SDMP
1878.71 cm = SUML for ILP8
1905.7 cm = SUML for BX02
2017.44 cm = SUML for IM03